KINEMATIC ANALYSIS OF A THREE DEGREES OF FREEDOM IN-PARALLEL ACTUATED MANIPULATOR

Kok-Meng Lee and Dharmen K. Shah

The George W. Woodruff School of Mechanical Engineering
Georgia Institute of Technology
Atlanta, Georgia 30332

Abstract

This paper presents an alternative design of a three degrees of freedom manipulator based on the concept of in-parallel actuated mechanism. The manipulator has two degrees of orientation freedom and one degree of translatory freedom. The basic kinematic equations for use of the manipulator are derived and the influences of the physical constraints on the range of motion in the practical design are discussed. Several possible applications which include the in-parallel mechanism as part of the manipulation system are suggested.

Introduction

Industrial robots have traditionally been used as general-purpose positioning devices and are anthropomorphic open chain mechanisms which generally have the links actuated in series. The open kinematic chain manipulators usually have longer reach, larger workspace and more dextrous maneuverability in reaching small space. However, the cantilever-like manipulator is inherently not very rigid and has poor dynamic performance at high speed and high dynamic loading operating conditions.

Recently, some efforts have been directed towards the investigation of alternative manipulator designs based on the concepts of closed kinematic chain due to the following advantages as compared to the traditional open kinematic chain manipulators; namely, more rigid and accurate due to the lack of cantilever-like structure, high force/torque capacity for the number of actuators as the actuators are arranged in parallel rather than in series, and relatively simpler inverse kinematics which is an advantage in real-time on-line computer control. The closed kinematic chain manipulators have potential applications where the demand on workspace and maneuverability is low but the dynamic loading is severe and high speed and precision motion are of primary concerns. Typical examples of in-parallel mechanism are camera tripod and six degrees of freedom Steward platform which is originally designed as an aircraft simulator[1] and later as a robot wrist[2]. Various applications of the Steward platform have been investigated for use in mechanized assembly and for use as a compliance device[3]. Significant effort has been directed towards tendon actuated in-parallel manipulators[4,5] which have the advantages of high force to weight ratio. A systematic review on possible alternative in-parallel mechanisms and other combinations in which part of the manipulator is serial and part parallel have been addressed by Hunt[6] and by Fichter and McDowell[7]. The kinematics and practical design consideration have been discussed in technical literature[8,9].

The manipulation approach analyzed in this paper is based on an in-parallel actuated tripod-like manipulator which has two degrees of orientation freedom and one degree of translatory freedom. The purpose of this investigation is to develop an analytical method and systematic design procedures to analyze the basic kinematics. The influences of the physical constraints on the practical design imposed by the limits of the ball joints and the links on the kinematics are discussed.

Kinematics equations for the three degrees of freedom in-parallel actuated manipulator

A schematic of an in-parallel manipulator is shown in Fig. 1. The manipulator consists of an upper platform which houses the driving mechanism of the gripper, three extensible links and a base platform. The upper platform is connected to the links by means of ball joints which are equally spaced at 120 degrees and at a radius r from the center of the upper platform. The other ends of the links are connected to the base platform through equally spaced pin joints at a radius R from the center of the base platform. By varying the link lengths, the upper platform can be manipulated with respect to the base platform.

A base cartesian co-ordinate frame XYZ is fixed at the center of the base platform with the Z axis pointing vertically upward and the X axis pointing towards the pin joint 1, P_1. Similarly, a co-ordinate frame xyz is assigned to the center of the upper platform, with the z axis normal to the platform and the x axis pointing towards the ball joint 1, B_1. Hence, the coordinates of the pin joints in XYZ frame are:

$$\mathbf{P_1} = \begin{bmatrix} R \\ 0 \\ 0 \end{bmatrix} \quad \mathbf{P_2} = \begin{bmatrix} -\frac{1}{2}R \\ \frac{\sqrt{3}}{2}R \\ 0 \end{bmatrix} \quad \mathbf{P_3} = \begin{bmatrix} -\frac{1}{2}R \\ -\frac{\sqrt{3}}{2}R \\ 0 \end{bmatrix} \qquad (1)$$

CH2413-3/87/0000/0345$01.00 © 1987 IEEE

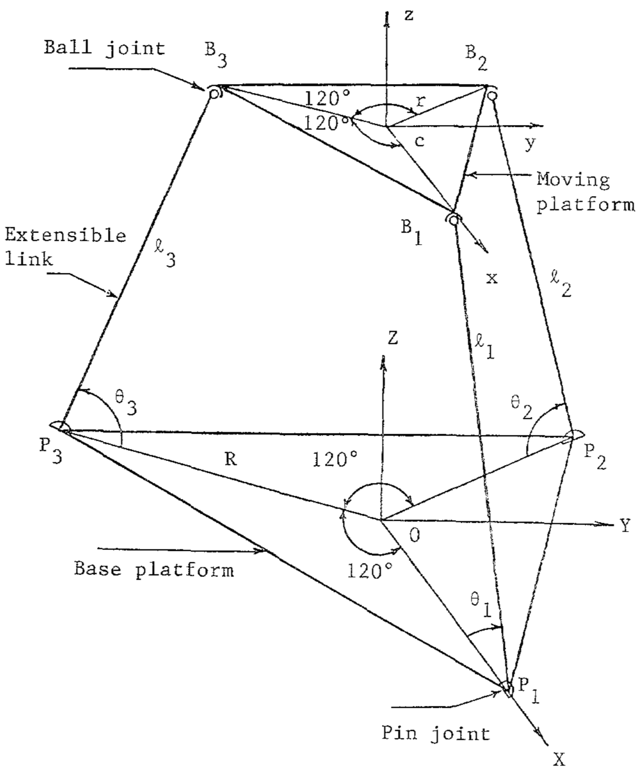

Figure 1. Schematic of a 3 degree-of-freedom in-parallel actuated mechanism

and coordinates of the ball joints in xyz frame are:

$$\mathbf{b_1} = \begin{bmatrix} r \\ 0 \\ 0 \end{bmatrix} \quad \mathbf{b_2} = \begin{bmatrix} -\frac{1}{2}r \\ \frac{\sqrt{3}}{2}r \\ 0 \end{bmatrix} \quad \mathbf{b_3} = \begin{bmatrix} -\frac{1}{2}r \\ -\frac{\sqrt{3}}{2}r \\ 0 \end{bmatrix} \qquad (2)$$

The coordinate frame xyz with respect to the base coordinate frame XYZ can be described by the homogeneous transformation [T]:

$$[T] = \begin{bmatrix} n_1 & o_1 & a_1 & x_c \\ n_2 & o_2 & a_2 & y_c \\ n_3 & o_3 & a_3 & z_c \\ 0 & 0 & 0 & 1 \end{bmatrix} \qquad (3)$$

where $(x_c, y_c, z_c)^T$ describes the position of the origin of the xyz frame and the orientation vectors $(n_1, n_2, n_3)^T$, $(o_1, o_2, o_3)^T$ and $(a_1, a_2, a_3)^T$ are the directional cosines of the axes x, y and z with respect to the base frame XYZ. As the unit vectors $\underline{n}$, $\underline{o}$ and $\underline{a}$ form a orthonormal set, there are six constraint equations on the nine elements, i.e.

$$\left.\begin{array}{l} \underline{n}\cdot\underline{n} = \underline{o}\cdot\underline{o} = \underline{a}\cdot\underline{a} = 1 \\ \underline{o}\cdot\underline{a} = \underline{o}\cdot\underline{n} = \underline{a}\cdot\underline{n} = 0 \end{array}\right\} \qquad (4)$$

The cartesian position of the ball joints with respect to the base frame XYZ can be expressed as:

$$\begin{bmatrix} \mathbf{B_i} \\ 1 \end{bmatrix}_{XYZ} = [T] \begin{bmatrix} \mathbf{b_i} \\ 1 \end{bmatrix}_{xyz} \qquad (5)$$

where the vectors $\mathbf{B_i}$ and $\mathbf{b_i}$ describe the position vectors of ith ball joint with respect to the base frame XYZ and frame xyz respectively. The length of the link, which is equal to the distance between the ith ball joint and the ith pin joint, is:

$$L_1^2 = (n_1\rho + X_c - 1)^2 + (n_2\rho + Y_c)^2 + (n_3\rho + Z_c)^2 \qquad (6)$$

$$L_2^2 = \frac{1}{4}[(-n_1\rho + \sqrt{3}\,o_1\rho + 2X_c + 1)^2 + (-n_2\rho + \sqrt{3}\,o_2\rho + 2Y_c - \sqrt{3})^2 + (-n_3\rho + \sqrt{3}\,o_3\rho + 2Z_c)^2] \qquad (7)$$

$$L_3^2 = \frac{1}{4}[(-n_1\rho - \sqrt{3}\,o_1\rho + 2X_c + 1)^2 + (-n_2\rho - \sqrt{3}\,o_2\rho + 2Y_c + \sqrt{3})^2 + (-n_3\rho - \sqrt{3}\,o_3\rho + 2Z_c)^2] \qquad (8)$$

where $\rho = \frac{r}{R}$,

$$L_i = \frac{\ell_i}{R}, \qquad i = 1, 2, 3$$

$$X_c = \frac{x_c}{R}, \qquad Y_c = \frac{y_c}{R}, \qquad Z_c = \frac{z_c}{R}$$

As the links P_1B_1, P_2B_2 and P_3B_3 are constrained by the pin joints to move in the planes, y = 0, $y = -\sqrt{3}\,x$ and $y = +\sqrt{3}\,x$ respectively, the constraint equations imposed by the pin joints are,

$$o_2\rho + Y_c = 0 \qquad (9)$$

$$-n_2\rho + \sqrt{3}\,o_2\rho + 2Y_c = -\sqrt{3}\,[-n_1\rho + \sqrt{3}\,o_1\rho + 2X_c] \qquad (10)$$

$$-n_2\rho - \sqrt{3}\,o_2\rho + 2Y_c = \sqrt{3}\,[-n_1\rho - \sqrt{3}\,o_1\rho + 2X_c] \qquad (11)$$

By adding Equations (10) and (11) and subtracting Equation (10) from Equation (11) respectively, the constraint equations (10) and (11) can be simplified as:

$$n_2 = o_1 \tag{12}$$

$$X_c = \frac{\rho}{2}(n_1 - o_2) \tag{13}$$

As Equation (12) imposes an orientation constraint in addition to that described in Equation (4), therefore only two of nine directional cosines are independent. Equations (9) and (13) relates X_c and Y_c to the directional cosines. Hence, the manipulator has only two freedoms in orientation and one freedom in cartesian position.

Equations (6), (7) and (8) are the inverse kinematic equations which define the actuating length of the links for a prescribed position and orientation of the moving platform. To compute the link lengths using Equations (6) - (8), both the position and orientation of the moving frame, i.e. six variables, must be defined. As the system has three degrees of freedom, only three of the six position/orientation variables are independent and the remaining dependent variables must be calculated from Equations (5), (9), (12) and (13).

A more compact form of solutions for the link lengths can be obtained by expressing the directional cosines in terms of Z-Y-Z Euler angles (α, β, γ)[10] as:

$$\alpha = \mathrm{Atan2}(a_2, a_1) \tag{14}$$

$$\beta = \mathrm{Atan2}(\sqrt{n_3^2 + o_3^2}, a_3) \tag{15}$$

$$\gamma = \mathrm{Atan2}(o_3, -n_1) \tag{16}$$

where $0 < \beta < \pi$.

Equation (12) becomes:

$$\alpha + \gamma = n\pi \qquad n = 0, \pm 1, \pm 2. \tag{17}$$

Mathematically, two possible sets of link lengths for a specified set of α, β and Z_c can be obtained depending on whether n is even or odd. As there are physical constraints imposed by the limits of the ball joints, only n equal to zero is physically realizable. Hence, Equations (13) and (9) becomes

$$X_c = -\frac{1}{2}\rho(1 - C_\beta)C_{2\alpha} \tag{18}$$

$$Y_c = \frac{1}{2}\rho(1 - C_\beta)S_{2\alpha} \tag{19}$$

where $C_\beta = \cos\beta$, $S_{2\alpha} = \sin 2\alpha$, and $C_{2\alpha} = \cos 2\alpha$. The cartesian position, X_c and Y_c, can be expressed graphically as a function of α and β. The constant $\cos\beta$ plots are essentially a family of concentric circles with the radii linearly proportional to trigonometric cosines of β and the constant α plots are a family of straight radial lines originating from the origin with the slopes equal to $\tan(-2\alpha)$. The algebraic sign of X_c and Y_c depends on the value of 2α.

The link lengths in terms of Euler angles are:

$$\begin{aligned} L_1^2 = {} & 1 + \rho^2 + X_c^2 + Y_c^2 + Z_c^2 - 2X_c \\ & + 2\rho\,(C_\alpha^2 C_\beta + S_\alpha^2)(X_c - 1) \\ & + \rho\,(C_\beta - 1)S_{2\alpha}Y_c - 2\rho\, S_\beta\, C_\alpha\, Z_c \end{aligned} \tag{20}$$

$$\begin{aligned} L_2^2 = {} & 1 + \rho^2 + X_c^2 + Y_c^2 + Z_c^2 + X_c - \sqrt{3}\,Y_c \\ & - \rho[C_\alpha^2 C_\beta + S_\alpha^2 - \sqrt{3}\,C_\alpha S_\alpha(C_\beta - 1)][X_c + \tfrac{1}{2}] \\ & - \rho[S_\alpha C_\alpha(C_\beta - 1) - \sqrt{3}\,(S_\alpha^2 C_\beta + C_\alpha^2)][Y_c + \tfrac{\sqrt{3}}{2}] \\ & + \rho\, S_\beta\,[C_\alpha - \sqrt{3}\,S_\alpha]\, Z_c \end{aligned} \tag{21}$$

$$\begin{aligned} L_3^2 = {} & 1 + \rho^2 + X_c^2 + Y_c^2 + Z_c^2 + X_c + \sqrt{3}\,Y_c \\ & - \rho[C_\alpha^2 C_\beta + S_\alpha^2 + \sqrt{3}\,C_\alpha S_\alpha\,(C_\beta - 1)][X_c + \tfrac{1}{2}] \\ & - \rho[S_\alpha C_\alpha(C_\beta - 1) + \sqrt{3}\,(S_\alpha^2 C_\beta + C_\alpha^2)][Y_c + \tfrac{\sqrt{3}}{2}] \\ & + \rho\, S_\beta[C_\alpha + \sqrt{3}\,S_\alpha]\, Z_c \end{aligned} \tag{22}$$

where $S_\alpha = \sin\alpha$, $C_\alpha = \cos\alpha$ and $S_\beta = \sin\beta$. Hence, the independent variables are α, β and Z_c and the dependent variables γ, X_c and Y_c are defined in Equations (17), (18) and (19) respectively.

Forward Kinematics

The inverse kinematic discussed in previous section must generally be computed on-line for real time trajectory control of the manipulator. In dynamic analysis of the manipulator, both the forward kinematic which transforms the given actuator coordinates to cartesian coordinates and the inverse kinematic are necessary. The forward kinematic involves solving the six simultaneous equations for the position/orientation in terms of the given line lengths. An alternative method to solve for the forward kinematics can be derived by noting the fact that the in-parallel actuated manipulator is essentially a structure for given link lengths.

The angles θ_1, θ_2 and θ_3 are defined to be the angles between the links L_1, L_2 and L_3 and the base platform respectively. As the distance between any two adjacent ball joints is $\sqrt{3}\,r$, θ_i can be related to L_i implicitly using Equation (5) as:

$$L_1^2 + L_2^2 + 3 - 3\rho^2 + L_1L_2 \cos\theta_1 \cos\theta_2 - 2L_1L - 3L_1 \cos\theta_1 - 3L_2 \cos\theta_2 = 0 \quad (23)$$

$$L_2^2 + L_3^2 + 3 - 3\rho^2 + L_2L_3 \cos\theta_2 \cos\theta_3 - 2L_2L - 3L_2 \cos\theta_2 - 3L_3 \cos\theta_3 = 0 \quad (24)$$

$$L_3^2 + L_1^2 + 3 - 3\rho^2 + L_3L_1 \cos\theta_3 \cos\theta_1 - 2L_3 - 3L_3 \cos\theta_3 - 3L_1 \cos\theta_1 = 0 \quad (25)$$

where the coordinates of the ball joints with respect to the base frame are:

$$\left.\begin{aligned} X_{b1} &= 1 - L_1 \cos\theta_1 \\ Y_{b1} &= 0 \\ Z_{b1} &= L_1 \sin\theta_1 \end{aligned}\right\} \quad (26)$$

$$\left.\begin{aligned} X_{b2} &= -\frac{1}{2}(1 - L_2 \cos\theta_2) \\ Y_{b2} &= +\frac{\sqrt{3}}{2}(1 - L_2 \cos\theta_2) \\ Z_{b2} &= L_2 \sin\theta_2 \end{aligned}\right\} \quad (27)$$

$$\left.\begin{aligned} X_{b3} &= -\frac{1}{2}(1 - L_3 \cos\theta_3) \\ Y_{b3} &= -\frac{\sqrt{3}}{2}(1 - L_3 \cos\theta_3) \\ Z_{b3} &= L_3 \sin\theta_3 \end{aligned}\right\} \quad (28)$$

As the ball joints are placed at the vertices of an equilateral triangle, the cartesian position or the origin of the moving frame, which is essentially the centroid of the triangle, can be determined as:

$$\left.\begin{aligned} X_c &= \frac{1}{3} \sum_{i=1}^{3} \frac{x_{bi}}{R} \\ Y_c &= \frac{1}{3} \sum_{i=1}^{3} \frac{y_{bi}}{R} \\ Z_c &= \frac{1}{3} \sum_{i=1}^{3} \frac{z_{bi}}{R} \end{aligned}\right\} \quad (29)$$

The orientation can be calculated using Equations (17) - (19).

Physical Constraints

The equations derived above are for the general position/orientation of the moving platform. However, in the design of a practical manipulator, there are physical constraints such as the limits of the ball joints and the actuating link lengths. Unlike the constraints imposed by the pin joints which limit the effective degrees of freedom, the physical constrains discussed in this section primarily limit the range of motion.

Fig. 2 shows a typical cross-section of

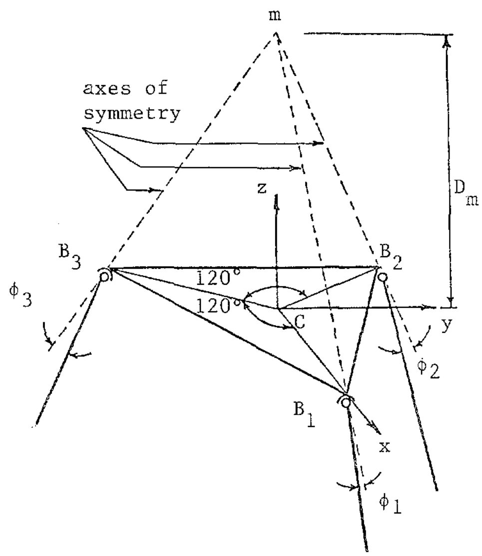

Figure 2. Schematic of the ball joints with respect to moving platform.

ball and socket joints where ϕ_i is the angle between the axis of symmetry of the ball joint and the link. The maximum angle of ball joints, ϕ_{max}, has significant influence on the orientation of moving platform. The following derivation aims to express the angle ϕ_i as a function of the cartesian position/orientation of the moving platform. If the normal vector, $\underline{N}$, of a plane containing the ball joints is:

$$\underline{N} = C_1\underline{I} + C_2\underline{J} + C_3\underline{K} \quad (30)$$

and the equation of the corresponding plane is:

$$A_1x + A_2y + A_3z = d \quad (31)$$

we have

$$\underline{N} = \overline{B_1B_2} \times \overline{B_2B_3} \quad (32)$$

where B_1B_2 and B_2B_3 are the line vectors directed from ball joints B1 to B2 and B2 to B3 respectively. With the cartesian coordinates of the ball joints given in Equations (5), the components of the normal vector $\underline{N}$ can then be determined as:

$$\left.\begin{aligned} C_1 &= \frac{3\sqrt{3}}{2} r^2(n_2o_3 - o_2n_3) \\ C_2 &= \frac{3\sqrt{3}}{2} r^2(-n_1o_3 + o_1n_3) \\ C_3 &= \frac{3\sqrt{3}}{2} r^2(n_1o_2 - o_1n_2) \end{aligned}\right\} \quad (33)$$

As the sockets of the ball joints are rigidly attached to the moving platform, the axis of symmetry of each socket intersects the normal of the plane at m. The equation of the line along the normal and passing through the point (x_c, y_c and z_c) is:

$$\frac{x - x_c}{C_1} = \frac{y - y_c}{C_2} = \frac{z - z_c}{C_3} \qquad (34)$$

By defining the unit vector components such that:

$$A_i = \frac{C_i}{\sqrt{C_1^2 + C_2^2 + C_3^2}} \qquad i = 1,\ 2,\ 3 \qquad (35)$$

Equation (34) can be re-written as:

$$\frac{x_m - x_c}{A_1} = \frac{y_m - y_c}{A_2} = \frac{z_m - z_c}{A_3} = D_m \qquad (36)$$

Hence, the cartesian coordinates of m can be obtained as:

$$\left.\begin{aligned} x_m &= x_c + A_1 D_m \\ y_m &= y_c + A_2 D_m \\ z_m &= z_c + A_3 D_m \end{aligned}\right\} \qquad (37)$$

Similarly, the equation of the line passing through ith ball joint and ith pin joint is:

$$\frac{x - x_{pi}}{x_{bi} - x_{pi}} = \frac{y - y_{pi}}{y_{bi} - y_{pi}} = \frac{z - z_{pi}}{z_{bi} - z_{pi}} \qquad (38)$$

where i = 1,2,3.

Hence, the angle between the lines described by Equations (34) and (38) is:

$$\cos \phi_i = \frac{1}{\sqrt{(x_{bi} - x_{pi})^2 + (y_{bi} - y_{pi})^2 + (z_{bi} - z_{pi})^2}} \cdot \frac{1}{\sqrt{(x_m - x_{bi})^2 + (y_m - y_{bi})^2 + (z_m - z_{bi})^2}} \cdot$$
$$[(x_m - x_{bi})(x_{bi} - x_{pi}) + (y_m - y_{bi})(y_{bi} - y_{pi}) + (z_m - a_{bi})(z_{bi} - z_{pi})] \qquad (39)$$

where i = 1, 2, 3 and $0 < \phi_i < \phi_{max}/2$.

A simulation of the kinematics of the three degrees of freedom in-parallel actuated manipulator has been written to investigate the range of motion limited by the ball joints and the links. The simulation is done for an X-Y plane with Z_c held constant. The simulation shows the extremes of the X_c and Y_c for a given design. An example of the simulation output is shown in Fig. 3 for the following configuration. Minimum and maximum link lengths are R and 3R respectively, ϕ_{max} is 45 degrees and D_m = 1.75.

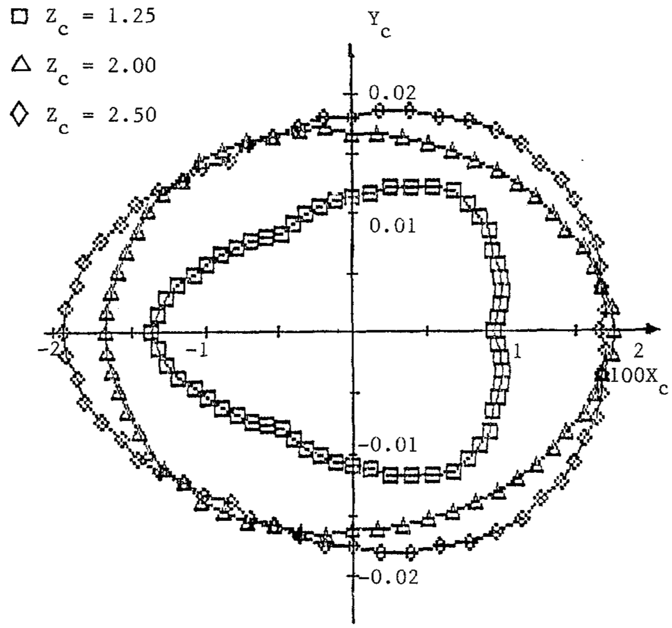

Figure 3. X-Y plots of the work envelope of the in-parallel actuated mechanism.

It is noted that the range of motion is primarily limited by the maximum angle of the ball joints except in the proximity of the minimum and maximum Z_c. Fig. 4 shows that the value of D_m has a significant influence on the size and shape of the work envelop. The simulation output is useful in determining the range of motion and understanding the size and shape of work envelop. It also serves as a means of sizing the practical design parameters.

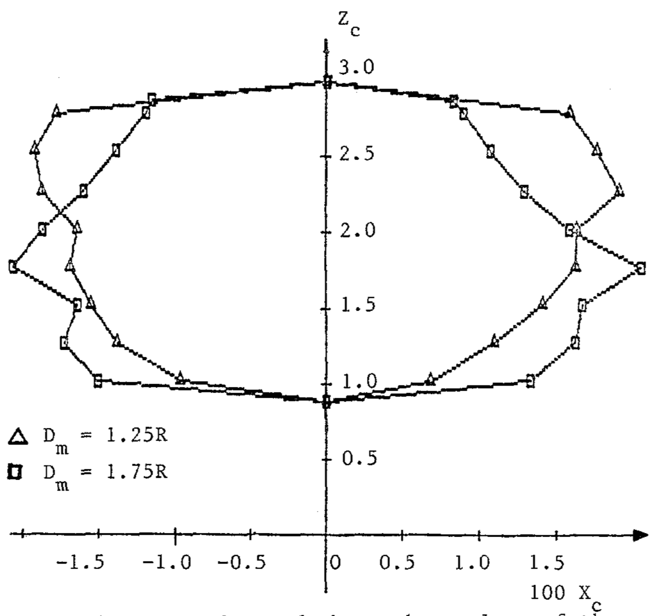

Figure 4a. X-Z plots of the work envelope of the in-parallel actuated mechanism.

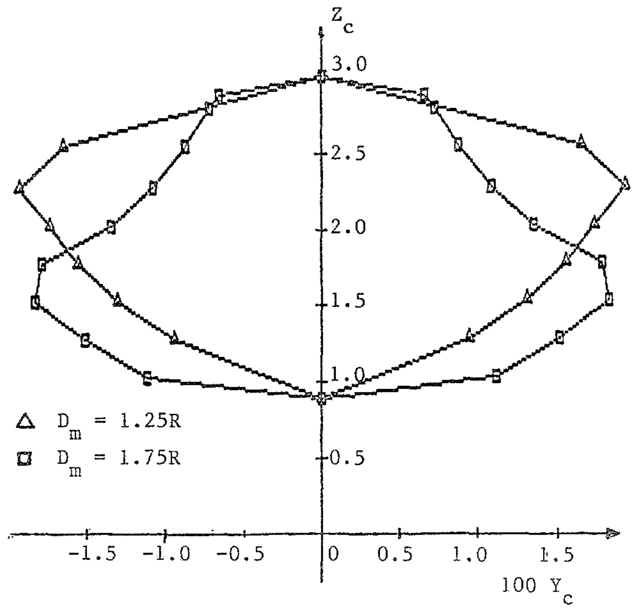

Figure 4b. Y-Z plots of the work envelope of the in-parallel actuated mechanism.

Applications

The in-parallel manipulator has potential applications where the orientation and reach in Z direction are more important than the translation in X and Y direction. Apart from the suggestion made by Hunt[10] that a six degrees of freedom arm could comprise two three degrees of freedom in-parallel actuated arms connected in series with one another, the following are two practical applications of the manipulator as part of the six degrees of freedom manipulation systems. It is noted that with an additional rotational freedom provided by the spin actuator and that the translations in X and Y directions obtainable by means of an X-Y table or cartesian manipulator, the attractive features of an in-parallel actuated mechanism can be achieved without sacrificing the work space. Typical applications are automated assembly, contour machining and material handling. A manipulator may consist of an in-parallel actuated mechanism and a spherical wrist motor[11] to form a six degrees of freedom dexterous end effector.

Conclusion

This paper presents the kinematic equations for use of a three degrees of freedom in-parallel actuated mechanism as a robot manipulator. The physical constraints imposed by the limits of the ball joints and the link lengths have been discussed. A simulation program has been developed to predict the range of motion for the purpose of practical design. Various possible applications of the in-parallel mechanism as part of the six degrees of freedom manipulator are addressed. Future work includes dynamic analysis, prototype design and evaluation in an industrial environment and computer control scheme development.

Acknowledgments

We would like to express our thanks to Georgia Institute of Technology for support from the general research fund and from the Computer Integrated Manufacturing Systems (CIMS) Program and to Dr. Wayne Book, CIMS Director, for establishing our contact with the CIMS program and for providing a stimulating research environment.

References

[1] D. Stewart, "A Platform with Six Degrees of Freedom," Proceedings of the Institute of Mechanical Engineers, Vol. 180, Part 1, no. 15, 1965-66, pp. 371-386.

[2] Bennett, "A Mechanical Wrist for a Robot Arm," B. S. Thesis, MIT 1968.

[3] H. McCallian and P. D. Truceng, "The Analysis of a Six-Degree-of-Freedom Work Station for Mechanized Assembly," Proceedings of the Fifth World Congress for the Theory of Machines and Mechanisms, An ASME Publication, 1979, pp. 611-616.

[4] K. H. Lim, "Control of a Tendon Arm," MIT A. I. Memo, No. 617, February 1981.

[5] S. E. Landsberger, "Design and Construction of a Cable-Controlled, Parallel Link Manipulator, MIT S. M. Thesis, September 1984.

[6] K. H. Hunt, "Structural Kinematics of In-Parallel-actuated Robot Arms.", Trans. ASME, J. Mechanisms, Transmissions, and Automation in Design 105: 705-712, 1983.

[7] E. F. Fichter and E. D. McDowell, "A Novel Design for a Robot Arm," Advances in Computer Technology, an ASME Publication, 1980, pp. 250-256.

[8] D. C. H. Yang and T. W. Lee, "Feasibility Study of a Platform Type of Robotic Manipulators from a Kinematic Viewpoint," Journal of Mechanisms Transmissions, and Automation in Design, June 1984, Vol. 106, pp. 191-198.

[9] E. F. Fichter, "A Steward Platform-Based Manipulator: General Theory and Practical Construction," The International Journal of Robotics Research, Vol. 5, No. 2, Summer 1986.

[10] J. J. Craig, "Introduction to Robotics, Mechanics and Control," Addison-Wesley Publishing Company, 1985.

[11] K. Davey and G. Vachtesevanos, "The Analysis of Fields and Torques in a Spherical Induction Motor, IEEE Trans. Mag., Sept. 1986.